

# Metabolic Imaging with Gallium-68- and Indium-111-Labeled Low-Density Lipoprotein

Stephen M. Moerlein, Alan Daugherty, Burton E. Sobel, and Michael J. Welch

*The Edward Mallinckrodt Institute of Radiology, Department of Biochemistry and Molecular Biophysics, and Department of Medicine, Washington University School of Medicine, St. Louis, Missouri*

Low-density lipoprotein (LDL) labeled with either gallium-68 ( $^{68}\text{Ga}$ ) or indium-111 ( $^{111}\text{In}$ ) was evaluated as a potential PET or SPECT radiopharmaceutical for determination of hepatic lipoprotein metabolism in rabbits. Gallium-68 or  $^{111}\text{In}$  was linked to LDL via diethylenetriaminepentaacetic acid (DTPA) with a 25–70% radiochemical yield. Studies in vivo that compared  $^{68}\text{Ga}$ - or  $^{111}\text{In}$ -DTPA-LDL with dilactitol- $^{125}\text{I}$ -tyramine LDL and  $^{131}\text{I}$ -LDL showed that both  $^{68}\text{Ga}$ - and  $^{111}\text{In}$ -labeled LDL behaved as residualizing radiotracers. Localization of radioactivity within the liver of normal rabbits was visualized clearly with [ $^{68}\text{Ga}$ ]DTPA-LDL by PET and with [ $^{111}\text{In}$ ]DTPA-LDL by gamma scintigraphy. Significant differences were observed in hepatic uptake of normal compared with hypercholesterolemic rabbits in which low-capacity LDL receptor-mediated catabolism was saturated. Gallium-68 and  $^{111}\text{In}$ -DTPA-LDL are attractive radiopharmaceuticals for noninvasive delineation of tissue LDL metabolism under normal and pathophysiological conditions.

**J Nucl Med 1991; 32:300–307**

**E**levated plasma concentrations of low-density lipoprotein (LDL) predispose to atherogenesis and coronary heart disease (1–3). Conventional therapeutic approaches to normalizing plasma lipids entail both dietary and pharmacologic measures (4–6) and are thought to favorably modify the saturable, receptor-mediated metabolism of LDL (7–8). Although loci of metabolism of lipoproteins in tissues have been delineated in vitro with cell culture techniques, studies of their metabolism in tissues of intact organisms have been limited because of the need for invasive procedures.

Lipoprotein catabolism has been evaluated in vivo with iodine-123- ( $^{123}\text{I}$ ) labeled very-low density lipoprotein (VLDL) used as a tracer (9). Although the importance of hepatic LDL receptors has been documented clearly, quantification of catabolism in tissues has not been possible because of rapid leakage of radioactive

catabolites from their site of origin. Use of LDL labeled with the residualizing label cellobiitol- $^{123}\text{I}$ -tyramine (TC) circumvented this difficulty because the tracer remained trapped intracellularly within tissues despite metabolic degradation of the lipoprotein (10). LDL labeled with technetium-99m has been used as well (11,12). Its biodistribution profile resembles that of  $^{123}\text{I}$ -TC-LDL (12).

The present study was designed to assess the utility of LDL radiolabeled with gallium-68 ( $^{68}\text{Ga}$ ) ( $\beta^+$ ,  $t_{1/2} = 68$  min) or indium-111 ( $^{111}\text{In}$ ) (173, 247 keV  $\gamma$ ,  $t_{1/2} = 67$  hr) for the determination of LDL metabolism. Each radiometal was attached to LDL via the bifunctional chelate diethylenetriaminepentaacetic acid (DTPA). Preliminary results with both of these tracers have been reported recently (13–15).

## MATERIALS AND METHODS

### Rabbits

New Zealand rabbits (Boswells Farms, Pacific, MO) weighing 1.8–2.4 kg were used for biodistribution and scintigraphic experiments. Control rabbits were maintained on a standard laboratory diet (Ralston Purina, St. Louis, MO). Hypercholesterolemia was induced by feeding rabbits the standard laboratory diet supplemented with 2% wt/wt cholesterol (Ralston Test Diets, Richmond, IN) (16). Watanabe heritable hyperlipidemic (WHHL) rabbits that served as a source of LDL were obtained from a colony derived from animals supplied by Dr. J. L. Goldstein (University of Texas) and maintained at Washington University. Food and water were available to all animals *ad libitum*.

### Radiochemistry

LDL was isolated and purified from WHHL rabbit plasma as described previously (17). Based on results in a previous report (18), purified LDL was reacted with cyclic DTPA anhydride (cDTPAA; Sigma Chemical Company, St. Louis, MO) to form DTPA-LDL conjugates for radiolabeling with either  $^{68}\text{Ga}$  or  $^{111}\text{In}$ . Typically, 1–2 mg of cDTPAA was suspended in methylene chloride, and a volume of the suspension corresponding to the desired mass of anhydride was transferred to a 16 × 125 mm borosilicate test tube and dried under a stream of nitrogen. LDL (4–6 mg/ml) was added, the contents of the test tube were mixed, and the coupling reaction was incubated at room temperature for 30 min. DTPA-LDL was separated from noncoupled cDTPAA with use of Sepha-

Received Apr. 24, 1990; revision accepted Aug. 14, 1990.  
For reprints contact: Stephen M. Moerlein, PhD, Division of Radiation Sciences Box 8131, Mallinckrodt Institute of Radiology, Washington University Medical School, 510 S. Kingshighway Blvd., St. Louis, MO 63110.

dex G-50 gel permeation chromatography (two 10 × 50 mm spin columns in sequence; 2,000 g × 5 min).

Na<sup>125</sup>I and Na<sup>131</sup>I were purchased from ICN Radiochemicals (Irvine, CA) for production of dilactitol-[<sup>125</sup>I]-tyramine (DLT)-LDL and <sup>131</sup>I-LDL, respectively. LDL was labeled directly via electrophilic iodination with sodium [<sup>131</sup>I]iodide oxidized in situ by Iodogen® (Pierce, Rockford, IL) (19). Iodine-125-DLT-LDL was prepared by reductive amination as described previously (20), and separated from noncoupled <sup>125</sup>I-DLT and inorganic <sup>125</sup>I species by gel permeation chromatography (10 × 100 mm preparative grade Superose 12; Pharmacia, Piscataway, NJ). The radioiodinated lipoproteins were dialyzed overnight against 0.15 M NaCl in 1 mM EDTA (pH 8.2), with three changes of buffer. The specific activity was ~0.1 μCi/mg protein for <sup>131</sup>I-LDL and ~0.25 μCi/mg protein for <sup>125</sup>I-DLT-LDL.

For the production of <sup>68</sup>Ga-DTPA-LDL, <sup>68</sup>Ga was eluted from 100 mCi <sup>68</sup>Ge bonded to an SnO<sub>2</sub> column (DuPont Medical Products, Boston, MA) with 4 ml 1M HCl (21) boiled to dryness in a 16 × 125 mm borosilicate test tube under a stream of nitrogen, and re-dissolved in 1 ml 0.4 M NaOAc, pH 7.0. The buffered solution of <sup>68</sup>Ga activity was then added to 1 mg DTPA-LDL, mixed, and incubated at room temperature for 1–30 min. Chelated <sup>68</sup>Ga-DTPA-LDL was separated from non-protein bound <sup>68</sup>Ga by gel permeation chromatography (two 10 × 50 mm Sephadex G-50 spin columns in sequence; 2,000 g × 5 min). The effluent solution was subjected to sterile filtration (0.45 μ Millex-GV; Millipore, Bedford, MA) to yield <sup>68</sup>Ga-DTPA-LDL with a specific activity of 5–10 mCi/mg.

Indium-111-InCl<sub>3</sub> was obtained as a no-carrier-added solution (~350 mCi/ml) at pH 1–2 (Mallinckrodt Nuclear, St. Louis, MO). Indium-111-DTPA-LDL was produced by addition of 1–5 mCi [<sup>111</sup>In]indium chloride to 1 mg DTPA-LDL in 1 ml 0.4 M NaOAc, pH 7.0. After an incubation period of 1–30 min at ambient temperature, product <sup>111</sup>In-DTPA-LDL was isolated from non-chelated <sup>111</sup>In radioactivity via chromatography as described above. The specific activity of the final product was 1–4 mCi/mg.

Radiolabeled LDL was subjected to radio-HPLC as well as agarose gel electrophoresis for assurance of quality. For radio-HPLC, a 5 × 6000 mm TSK-GEL G5000-PW column (P. J. Cobert, St. Louis, MO) and a mobile phase of 0.15 M NaCl, 0.5 ml/min was used. The agarose gel electrophoresis procedure used has been described in detail (22).

#### Determination of the Kinetics of Clearance from Plasma

Iodine-131-LDL (~100 μCi), <sup>125</sup>I-DLT-LDL (~100 μCi), and <sup>68</sup>Ga- or <sup>111</sup>In-DTPA-LDL (0.5–5 mCi) (corresponding to a total apoprotein mass of less than 1 mg) were injected simultaneously via a marginal ear vein into control rabbits weighing ~2 kg. At selected intervals after injections, 1 ml of blood was collected from a marginal ear vein of the opposite ear with syringes containing 1.5 mg EDTA. The blood samples were centrifuged for 2 min in a microfuge, and 100 μl of the resulting plasma were incubated with 100 μl of 20% wt/vol trichloroacetic acid (TCA) for 30 min at 4°C. The TCA-treated samples were centrifuged again, the supernatant fractions decanted, and the percentage of the radioactivity in the precipitated protein pellets determined with a well-type γ-scintil-

lation detector. The TCA-precipitated radioactivity at each interval was calculated as a percentage of the corresponding value for 1 min after injection. The kinetic constants for clearance from plasma were calculated with RStrip® (MicroMath, Salt Lake City, UT).

The concentrations of total cholesterol in each plasma sample and in isolated lipoprotein fractions were determined with commercially-available enzyme kits (Wako Chemical Company, Dallas, TX). The protein mass of lipoprotein fractions was determined by the method of Lowry et al. (23), with the use of bovine serum albumin as standard. Size distributions of radiolabeled DTPA conjugates of LDL in the plasma samples were determined by radio-HPLC, as described above.

#### Tissue Biodistribution Studies

Radiolabeled LDL was injected into rabbits as described above. After a 2-hr (for <sup>68</sup>Ga-DTPA-LDL) or 24-hr (for <sup>111</sup>In-DTPA-LDL) interval, the animals were killed by i.v. administration of pentobarbital (120 mg/kg). The organs listed in Table 1 were dissected free, lightly blotted, and weighed. Content of radioactivity was assayed with a well-type γ-scintillation counter. Results were calculated as percentages of the injected dose per gram of tissue per kilogram total body weight (% ID/kg/g) by comparison of the counts in tissue samples with those in a portion of the injected material.

#### Positron Emission Tomography

The distribution of <sup>68</sup>Ga-DTPA-LDL in vivo was measured noninvasively in normal and hypercholesterolemic rabbits with the use of SuperPET IIB, a whole-body time-of-flight positron tomograph with an in-plane reconstructed resolution of 12.2 mm (24). Rabbits were anesthetized with ketamine (30 mg/kg) and xylazine (60 mg/kg), and placed in a sagittal orientation within the rings of the tomograph so that normal and hypercholesterolemic animals could be imaged simultaneously. Transmission scans with a <sup>68</sup>Ge source were obtained for use in attenuation correction of the emission scans.

Gallium-68-DTPA-LDL (0.5 mCi, 0.5 mg) was administered by marginal ear vein injection simultaneously to anesthetized normal and hypercholesterolemic rabbits. Coincidence events were detected in a seven-slice, high-resolution acquisition mode. Data were reconstructed in sequential 30-

TABLE 1  
Tissue Biodistribution of <sup>68</sup>Ga-Labeled and Radioiodinated Analogues of LDL in Normal Rabbits\*

Tissue	Tissue concentration (%ID kg/g) <sup>†</sup>		
	<sup>131</sup> I-LDL	<sup>68</sup> Ga-DTPA-LDL	<sup>125</sup> I-DLT-LDL
Liver	0.18 ± 0.05	0.32 ± 0.06	0.30 ± 0.05
Spleen	0.15 ± 0.01	0.37 ± 0.05	0.33 ± 0.03
Adrenals	0.38 ± 0.09	0.37 ± 0.04	0.90 ± 0.26
Kidneys	0.19 ± 0.04	0.27 ± 0.04	0.18 ± 0.04
Muscle	0.03 ± 0.01	0.03 ± 0.02	0.02 ± 0.01
Plasma <sup>‡</sup>	1.36 ± 0.09	1.63 ± 0.13	1.77 ± 0.30

\* Two hours after injection.

<sup>†</sup> %ID kg/g = [counts in tissue/tissue mass (g)] + [total counts injected/total body mass (kg)] × 100%. Data are means ± standard errors (n = 4).

<sup>‡</sup> Data are %ID kg/ml.

min time intervals throughout the entire 120-min data collection. Regions of interest (ROI) were defined for the liver and cardiac blood pool. Decay-corrected data for each ROI were used to construct time-activity (cpm/voxel) relationships.

### Anger Camera Scintigraphy

Anesthetized rabbits were given [ $^{111}\text{In}$ ]DTPA-LDL (250  $\mu\text{Ci}$ , 0.5 mg) by marginal ear vein injection and the distribution of radioactivity imaged dynamically from a ventral direction. Anesthesia was maintained for 2 hr after injection for the initial 120-min imaging interval. For later imaging, rabbits were anesthetized again shortly before the imaging procedure. Images were obtained with an Anger camera equipped with a medium-energy, parallel-hole collimator. Energy discrimination was centered on the 247-keV photopeak of  $^{111}\text{In}$ , and collimator pixel dimensions of  $2.2 \times 2.2$  mm provided a system resolution of 2.5 mm FWHM at the collimator surface. Images of the abdomen of each rabbit included the liver, heart, spleen and lungs, and comprised at least  $10^5$  events. ROI were selected from the liver and the cardiac blood pool for construction of time-activity (cpm/ROI) curves.

## RESULTS

### Radiochemistry

The influence of the number of DTPA conjugates per LDL particle on the efficiency of  $^{68}\text{Ga}$  coordination is illustrated in Figure 1. Each point represents the mean of 2–3 determinations and indicates the percentage of total  $^{68}\text{Ga}$  activity in solution that was chelated by DTPA-LDL. Radiochemical yields are plotted as a function of the mean DTPA/LDL molar substitution ratio (SR). As SR was increased, labeling efficiency was enhanced. For a reaction interval of 30 min, the radiochemical yield of  $^{68}\text{Ga}$ -DTPA rose from approximately 10% for SR = 0.75 to approximately 50% for SR = 112. Because the impact of SR on the biochemical behavior or radiolabeled LDL in vivo was not known when this work was initiated, subsequent studies employed LDL conjugated at the level SR = 10, since radiochemical labeling provided convenient yields after short reaction intervals. A comparison of the radiola-

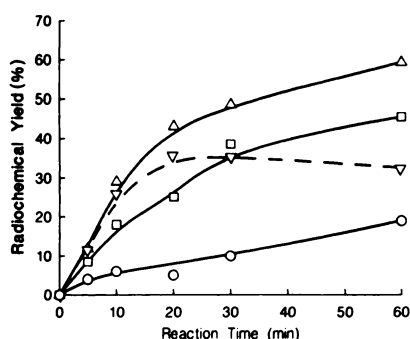


**FIGURE 1** Radiochemical yield of  $^{68}\text{Ga}$ -DTPA-LDL as a function of reaction interval and mean DTPA/LDL molar substitution ratio SR.  $\Delta$ , SR = 112;  $\square$ , SR = 11.5;  $\circ$ , SR = 0.75;  $\nabla$ , SR = 112 (non decay-corrected). Data are means of results from two to three experiments.

beling efficiency for reaction of  $^{68}\text{Ga}$  or  $^{111}\text{In}$  with DTPA-LDL was performed for SR = 10. Under these conditions, the radiochemical yield of  $^{111}\text{In}$ -DTPA-LDL exceeded that of  $^{68}\text{Ga}$ -DTPA-LDL by a factor of 6.5 at 5 min, and a factor of 2 after 30 min of reaction.

As judged from results of electrophoresis, native LDL migrated in the  $\beta$ -position, as expected. Both  $^{68}\text{Ga}$ -DTPA-LDL and  $^{111}\text{In}$ -DTPA-LDL exhibited the same mobility, indicating that neither the conjugation of DTPA nor subsequent coordination of tracer  $^{68}\text{Ga}$  or  $^{111}\text{In}$  introduced alterations in the charge characteristics of this lipoprotein fraction.

The results of radio-HPLC analyses of purified  $^{68}\text{Ga}$ - and  $^{111}\text{In}$ -DTPA-LDL conjugates show that the radiochemical purity of both radiotracers exceeded 97%. This fraction of the radioactivity co-eluted with native LDL on the size-exclusion HPLC column. The remaining fraction (<3%) of radioactivity eluted with the inclusion volume. It may reflect non-conjugated DTPA complexes or inorganic forms of the radiometals.

### Kinetics of Clearance

The clearance of  $^{68}\text{Ga}$ -DTPA-LDL and of  $^{111}\text{In}$ -DTPA-LDL from plasma is illustrated in Figure 2 along with corresponding data for  $^{131}\text{I}$ -LDL and  $^{125}\text{I}$ -DLT-LDL. Because of the short half-life of  $^{68}\text{Ga}$ , clearance curves for LDL labeled with this radioisotope were performed only in the first 2 hr after injection. Kinetics of clearance were similar for  $^{125}\text{I}$ -DLT-LDL,  $^{68}\text{Ga}$ - and  $^{111}\text{In}$ -DTPA-LDL, but clearance of the non-residualizing  $^{131}\text{I}$ -LDL was more rapid.

In 24-hr experiments, all radiolabeled analogues of LDL were eliminated from the plasma compartment in a biexponential manner. The fractional catabolic rate was calculated (25) to be  $0.119 \pm 0.017 \text{ hr}^{-1}$  and  $0.120 \pm 0.024 \text{ hr}^{-1}$  for  $^{125}\text{I}$ -DLT-LDL and  $^{111}\text{In}$ -DTPA-LDL, respectively. The fractional catabolic rate of  $^{131}\text{I}$ -LDL was slightly greater ( $0.174 \pm 0.016 \text{ hr}^{-1}$ ).

### Tissue Biodistribution Studies

Results of experiments designed to ascertain the tissue localization at autopsy of radiolabeled lipoprotein

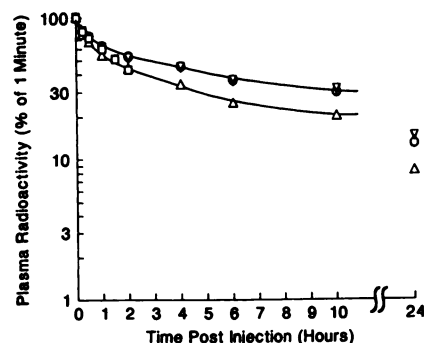


**FIGURE 2** Plasma clearance of radiolabeled analogues of LDL in rabbits.  $\square$ ,  $^{68}\text{Ga}$ -DTPA-LDL;  $\circ$ ,  $^{111}\text{In}$ -DTPA-LDL;  $\nabla$ ,  $^{125}\text{I}$ -DLT-LDL;  $\Delta$ ,  $^{131}\text{I}$ -LDL. Data are means of results from four or more animals.

**TABLE 2**  
Tissue Biodistribution of  $^{111}\text{In}$ -Labeled and Radioiodinated Analogues of LDL in Normal Rabbits\*

Tissue	Tissue concentration (%ID kg/g) <sup>†</sup>		
	$^{131}\text{I}$ -LDL	$^{111}\text{In}$ -DTPA-LDL	$^{125}\text{I}$ -DLT-LDL
Liver	0.26 ± 0.05	1.17 ± 0.22	1.56 ± 0.32
Spleen	0.71 ± 0.25	4.42 ± 0.85	3.49 ± 1.20
Adrenals	0.79 ± 0.25	4.78 ± 1.05	7.19 ± 2.01
Kidneys	0.18 ± 0.02	0.54 ± 0.05	0.33 ± 0.05
Plasma <sup>‡</sup>	0.34 ± 0.08	0.88 ± 0.22	1.00 ± 0.27

\* Twenty-four hours after injection.

<sup>†</sup> %ID kg/g = [counts in tissue/tissue mass (g)] + [total counts injected/total body mass (kg)] × 100%. Data are means ± standard errors (n = 4).

<sup>‡</sup> Data are %ID kg/ml.

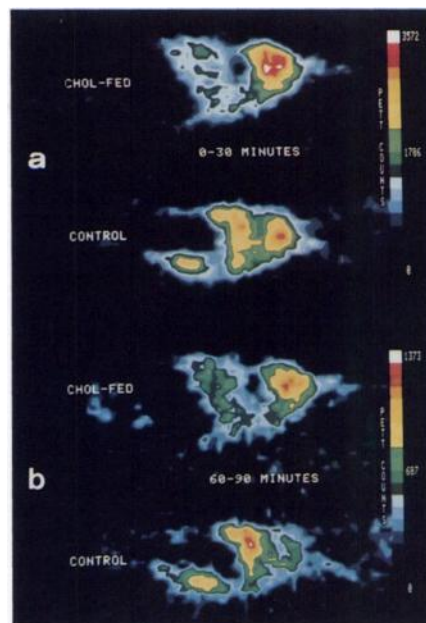
analogues in specific tissues are shown in Table 1 for  $^{68}\text{Ga}$ -DTPA-LDL and Table 2 for  $^{111}\text{In}$ -DTPA-LDL. The corresponding tissue localizations of residualizing metabolic tracer  $^{125}\text{I}$ -DLT-LDL and non-residualizing  $^{131}\text{I}$ -LDL are tabulated as well. Results are means and standard errors from four or more animals expressed as percentages of injected dose per gram of tissue per kilogram of total body weight (%ID kg/g) to correct for inter-animal differences arising solely from differences in body mass. Concentrations in tissues of  $^{68}\text{Ga}$ -DTPA-LDL were determined 2 hr after injection, whereas those of  $^{111}\text{In}$ -DTPA-LDL were evaluated 24 hr after administration of tracer. For both, the highest concentrations of radioactivity were in plasma, adrenals, spleen, and liver.

#### Positron Emission Tomography

Tomograms obtained simultaneously from a normal and a hypercholesterolemic rabbit given  $^{68}\text{Ga}$ -DTPA-LDL are shown in Figure 3. The section shown is a central sagittal one from each animal that includes the liver, heart, and spleen. Regional distribution of data from events detected throughout the interval from 0 to 30 min (Fig. 3a) or from 60 to 90 min (Fig. 3b) after injection of  $^{68}\text{Ga}$ -labeled lipoprotein after decay-correction to the time of injection are depicted. Localization of radioactivity in the liver of the normal rabbit is evident (lower tomograms). Hepatic sequestration of  $^{68}\text{Ga}$  activity is less distinct in the hypercholesterolemic animal (upper tomogram). The coincidence counts for liver and the thoracic blood-pool ROI were used to calculate relative uptake ratios R as a function of time after administration of  $^{68}\text{Ga}$ -DTPA-LDL as shown graphically in Figure 4.

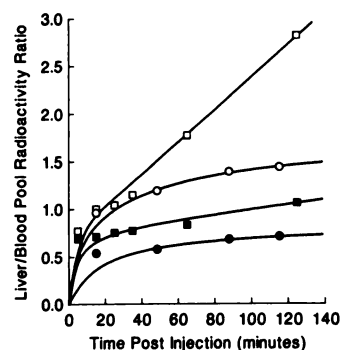
#### Anger Camera Scintigraphy

Figure 5 shows scintigraphic images of distribution of radioactivity 5 min, 2 hr, and 24 hrs after administration of  $^{111}\text{In}$ -DTPA-LDL to normal and hypercholesterolemic rabbits. Localization with the normal ani-



**FIGURE 3**  
Tomograms taken simultaneously from a hypercholesterolemic (upper) and normal (lower) rabbit administered  $^{68}\text{Ga}$ -DTPA-LDL. This central sagittal section includes the liver, heart, spleen, and kidneys. (a) 0–30 min after injection, (b) 60–90 min after injection of radiotracer.

mal was predominant in liver and considerable also in the spleen and kidneys. Images from the hypercholesterolemic rabbit illustrate modest accumulation of radioactivity in liver either 2 hr or 24 hr after injection of  $^{111}\text{In}$ -DTPA-LDL, consistent with diminished hepatic LDL receptor-mediated accumulation. Radioactivity sequestered in liver relative to that in the thoracic blood pool is illustrated in Figure 4. The ratio, R, of the counts detected in the liver ROI relative to the thoracic ROI was determined as a function of time after injection in the rabbits.



**FIGURE 4**  
Localization in vivo of  $^{68}\text{Ga}$ - and  $^{111}\text{In}$ -DTPA-LDL radioactivity in liver relative to that in the thoracic blood pool of rabbits as detected noninvasively by PET and gamma scintigraphy, respectively. Empty symbols, control rabbits; filled symbols, hypercholesterolemic rabbits. ○ and ●,  $^{68}\text{Ga}$ -DTPA-LDL. □ and ■,  $^{111}\text{In}$ -DTPA-LDL.

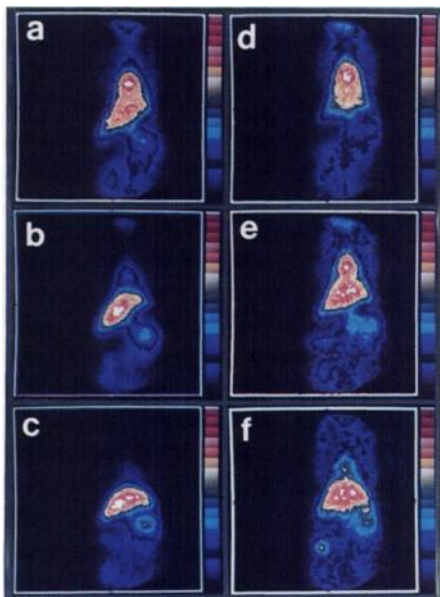


**FIGURE 5**  
Scintigrams taken from a normal (a–c) and hypercholesterolemic (d–f) rabbit given  $^{111}\text{In}$ -DTPA-LDL. Each image comprises events collected and summed over 10 min. (a) and (d), 0–10 min after injection; (b) and (e), 2 hr after injection; (c) and (f), 24 hr after injection of radiotracer.

## DISCUSSION

Determination of sites of lipoprotein metabolism in specific tissues *in vivo* has been limited in part by the biodegradable nature of conventional radiolabels. The recent development of radioiodinated residualizing protein labels such as dilactitol tyramine (DLT) (26) and cellobiitol-tyramine (TC) (27) has facilitated the evaluation of the catabolism of lipoproteins *in vivo*.

Although radioiodinated DLT and TC are generally considered to be optimal labels for tracers to define loci of lipoprotein catabolism *in vivo* in serial autopsy studies of groups of animals, the decay characteristics of iodine radioisotopes limit their widespread application for external detection. Iodine-123 decays via emission of a 159-keV gamma ray that can be imaged by gamma scintigraphy. However, its 13-hr half-life precludes universal, immediate availability of the radionuclide.

The group III radionuclides,  $^{68}\text{Ga}$  and  $^{111}\text{In}$ , have decay characteristics useful for nuclear medicine applications (28). Gallium-68 is a positron-emitting nuclide (90%  $\beta^+$ ,  $t_{1/2} = 68$  min) available from generators via decay of the 288-day half-lived  $^{68}\text{Ge}$  (21). Thus, PET studies can be performed on demand without a dedicated on-site cyclotron. Indium-111 decays with emission of a high flux (180%) of detectable photons. Its half-life of 2.8 days permits longer scanning intervals than those possible with other single-photon emitters and ease of distribution from production sites to nuclear medicine imaging facilities. Accordingly, we have eval-

uated the utility of both  $^{68}\text{Ga}$ - and  $^{111}\text{In}$ -labeled LDL as potential radiopharmaceuticals.

Gallium-68 and  $^{111}\text{In}$  exhibit similar coordination chemistry (28). Both were attached to LDL through DTPA conjugation. The radiochemical yields of  $^{111}\text{In}$ -DTPA-LDL were greater than those with  $^{68}\text{Ga}$ , probably because of residual acid remaining from the rapid drying of the 4 ml of 1 M HCl  $^{68}\text{Ge}/^{68}\text{Ga}$  generator eluate. The lower pH would be expected to decrease ionization and coordination by the DTPA groups on LDL. The  $<50 \mu\text{l}$  of pH 1–2 solvent containing  $^{111}\text{InCl}$  was unlikely to exceed the capacity of the buffer. Thus, greater ionization and coordination by DTPA of  $^{111}\text{In}$  was seen. The greater formation constant of DTPA for indium relative to gallium ( $\log K = 29.0$  and 25.54, respectively) (29) may have contributed to the higher radiochemical yields with  $^{111}\text{In}$ -DTPA-LDL.

Although production yields of  $^{68}\text{Ga}$ -DTPA-LDL were lower than those for  $^{111}\text{In}$ -DTPA-LDL, they were sufficient for applications *in vivo*. An important determinant for labeling with  $^{68}\text{Ga}$  was the 68-min half-life of the nuclide. When the nuclear decay factor was multiplied by the radiochemical yield of  $^{68}\text{Ga}$ -DTPA-LDL, the optimal exchange interval was found to be 20–30 min (Fig. 1). When this reaction time was employed, the radiochemical yield for  $^{68}\text{Ga}$ -DTPA-LDL was 24%–26% within an overall preparation and purification time of 55 min. For a 100-mCi  $^{68}\text{Ge}/^{68}\text{Ga}$  generator with an elution efficiency of 75%, this corresponds to an isolated product yield of 14.3 mCi.

The  $^{68}\text{Ga}$ - and  $^{111}\text{In}$ -DTPA-LDL analogues were very similar to native rabbit LDL. Both Sephadex gel permeation chromatography and agarose gel electrophoresis demonstrated migration patterns of radioactivity identical to those of unlabeled LDL. In each case, a single band of radioactivity indicating a radiochemical purity that exceeded 99% was evident. In addition, for the  $^{111}\text{In}$ -DTPA-LDL analogue, radiochemical purity exceeded 98% for as long as 10 days of storage at 4°C. The long shelf-life of  $^{111}\text{In}$ -DTPA-LDL is compatible with batch synthesis, storage, and distribution to remote sites.

Data obtained from studies *in vivo* suggest that the radiolabeled analogues had biologic behavior similar to that of unlabeled LDL. As shown in Figure 2, the clearance of both  $^{68}\text{Ga}$ - and  $^{111}\text{In}$ -DTPA-LDL was similar to that of the residualizing standard  $^{125}\text{I}$ -DLT-LDL. The calculated (25) fractional catabolic rates were also similar to that of native LDL (30). Thus, neither radiolabeling procedure altered essential biochemical determinants of clearance or catabolism of the lipoprotein particle.

The residualizing nature of the  $^{68}\text{Ga}$ - and  $^{111}\text{In}$ -DTPA conjugates was evident from results of the triple-label tissue biodistribution experiments. When the tissue retention of radioactivity from  $^{68}\text{Ga}$ -DTPA-LDL (Table

1) or  $^{111}\text{In}$ -DTPA-LDL (Table 2) was compared to that from residualizing  $^{125}\text{I}$ -DLT-LDL or metabolically labile  $^{131}\text{I}$ -LDL, it was evident that the radiometal-DTPA moieties were trapped *in vivo* in tissues with high lipoprotein catabolic activity. An example is the liver, the organ most abundant in LDL receptors (31) and the primary tissue for metabolism of lipoproteins (20,32). The hepatic content of radioactivity from  $^{131}\text{I}$ -LDL was relatively low because of the loss of the  $^{131}\text{I}$ -labeled metabolites generated by the enzymatic action of hepatocytes on the lipoprotein. The radioiodinated apolipoproteins are hydrolytically cleaved by lysosomes to iodotyrosine which cannot be used in any cellular processes and consequently is rapidly lost from the cell. In contrast, radioactivity from the  $^{68}\text{Ga}$ - or  $^{111}\text{In}$ -labeled analogues of LDL was retained in the liver in a manner similar to that of the residualizing carbohydrate label  $^{125}\text{I}$ -DLT. The retention may reflect enzymatic detachment of the DTPA-chelated metals from the lipoprotein or decomposition of the coordination compound within the intracellular space. In either case, the residualizing character of the  $^{68}\text{Ga}$ - or  $^{111}\text{In}$ -DTPA labels is a useful property because radioactivity that accumulates in tissues as a function of metabolic activity is retained in a stable fashion permitting detection by imaging procedures.

Localization of the radiopharmaceuticals in spleen and kidneys was modest, as was predicted from the biochemistry of LDL. For all organ compartments, the localization of radioactivity *in vivo* from  $^{68}\text{Ga}$ - or  $^{111}\text{In}$ -labeled LDL was similar to that of the residualizing  $^{125}\text{I}$ -DLT-LDL and much greater than that of the non-residualizing  $^{131}\text{I}$ -LDL.

Differences in the evaluation of tissue localization of  $^{68}\text{Ga}$ -DTPA-LDL and its  $^{111}\text{In}$  counterpart result from constraints placed by the half-lives of the radionuclides, as evident from the relative distribution of radioactivity in the liver and plasma compartments for  $^{68}\text{Ga}$ -DTPA-LDL after 2 hr (Table 1) and  $^{111}\text{In}$ -DTPA-LDL after 24 hr (Table 2). In the 22-hr difference between the applicable  $^{68}\text{Ga}$ - and  $^{111}\text{In}$ -DTPA-LDL intervals, radioactivity in the plasma pool decreased by approximately one-half (from approximately 60% to 30%) compared to that in the whole liver which doubled (from approximately 15% to 30%). Changes *in vivo* concur with the known 22-hr plasma clearance half-life of LDL (33) and are consistent with the hypothesis that the predominant pathway of elimination of the lipoprotein is hepatic catabolism.

In order to be useful as radiopharmaceuticals,  $^{68}\text{Ga}$ - and  $^{111}\text{In}$ -DTPA-LDL must satisfy two prerequisites. First, the target organ, in this case the LDL receptor-rich liver, must be clearly visualized within the temporal constraints defined by the half-life of the radionuclide. Second, the selective localization *in vivo* should change with alterations in metabolic state so that pathophysi-

ology can be elucidated by noninvasive imaging. A useful pathophysiologic paradigm of altered lipoprotein metabolism is saturation of low-capacity LDL receptors resulting from induced hypercholesterolemia (33). These requirements are satisfied with  $^{68}\text{Ga}$ -DTPA-LDL and PET as well as with  $^{111}\text{In}$ -DTPA-LDL and conventional  $\gamma$ -scintigraphy.

Localization of  $^{68}\text{Ga}$ -DTPA-LDL radioactivity within the liver was clearly detectable by positron tomography (Fig. 3). Radioactivity distributed equally in liver and the thoracic blood pool of the control rabbit from 0–30 min after injection (Fig. 3a, bottom), but hepatic sequestration of the  $^{68}\text{Ga}$ -labeled lipoprotein was distinct within 60–90 min (Fig. 3b, bottom). LDL receptors were saturated and/or down-regulated in the hypercholesterolemic rabbit, and uptake of radiotracer by liver was modest even after 60–90 min (Fig. 3b, top). Such changes can be mathematically indexed with respect to the ratio (R) of PET counts in the liver ROI relative to that in the thoracic blood-pool ROI. As shown in Figure 4, R for  $^{68}\text{Ga}$ -DTPA-LDL in the control rabbit increased to approximately 1.5 after 2 hr, in contrast to an R value of only 0.7 for the hypercholesterolemic rabbit.

Analogous data indicative of metabolism were obtained with  $^{111}\text{In}$ -DTPA-LDL and conventional gamma scintigraphic imaging equipment. Radioactivity clearly localized within the hepatic compartment of the control rabbit after 2 hr (Fig. 5b). After 24 hr, the majority of the radioactivity had residualized in the liver (Fig. 5c). These results contrast markedly with those from the hypercholesterolemic rabbit, in which a diffuse distribution of radioactivity was evident (Fig. 5d–f). These scintigraphic data were indexed with use of R values as noted above. As shown in Figure 4, after 130 min, R = 3 and 1 for  $^{111}\text{In}$ -DTPA-LDL in the normal and hypercholesterolemic rabbit, respectively. The greater R for  $^{111}\text{In}$ -DTPA-LDL relative to the  $^{68}\text{Ga}$ -labeled lipoprotein reflects the greater tissue depth of liver delineated by the Anger camera relative to the 14-mm tomographic slice quantified by the PET scanner. Imaging of the tissue biodistribution of  $^{111}\text{In}$ -DTPA-LDL 24 hr after injection distinguished normal from altered metabolic conditions even more strikingly; R was 7.5 for the control but only 1.6 for the hypercholesterolemic rabbit.

Compared with previously reported results with radiotracers in studies of lipoprotein metabolism,  $^{68}\text{Ga}$ - and  $^{111}\text{In}$ -DTPA-LDL have attractive characteristics as radiopharmaceuticals. Like LDL labeled with technetium-99m (10,33) or cellobiitol- $^{123}\text{I}$ -tyramine (10,11), both  $^{68}\text{Ga}$ - and  $^{111}\text{In}$ -labeled LDL have residualizing properties *in vivo*. Although the residualizing nature of  $^{111}\text{In}$ -DTPA-LDL was suggested in a previous report (15), in this work we have proven by direct comparison with  $^{125}\text{I}$ -DLT-LDL that both  $^{111}\text{In}$ - and  $^{68}\text{Ga}$ -labeled

LDL are intracellularly trapped in vivo. The long half-life of  $^{111}\text{In}$  relative to  $^{99\text{m}}\text{Tc}$  or  $^{123}\text{I}$  is advantageous for scintigraphic studies since imaging several days after injection is possible to yield R values even greater than those with the 24-hr data reported here. Despite the relatively modest R values for  $^{68}\text{Ga}$ -DTPA-LDL, this lipoprotein radiopharmaceutical can be used with PET for superior image resolution as well as absolute quantification of tracer disposition for kinetic modeling.

## CONCLUSIONS

Our results document the potential utility of  $^{68}\text{Ga}$ - and  $^{111}\text{In}$ -DTPA-LDL as radiopharmaceuticals for mapping loci of lipoprotein catabolism in vivo. The radiosynthesis of both tracers is facile, with radiochemical yields of 25% ( $^{68}\text{Ga}$ ) to 70% ( $^{111}\text{In}$ ) within a 1-hr preparation time. The labeling procedures employed do not affect characteristics of the lipoprotein particle essential for imaging applications. Biodistribution experiments that compared  $^{68}\text{Ga}$ - or  $^{111}\text{In}$ -labeled LDL with  $^{125}\text{I}$ -DLT-LDL or with  $^{131}\text{I}$ -LDL showed that the DTPA-radiometal conjugates behave in vivo like residualizing labels and that the labeled LDL derivatives are sequestered by LDL receptor-rich tissues. Most (62%–67% ID) of the radioactivity is confined to the plasma and hepatic compartments. The high (15%–30% ID) localization within liver augurs well for applications in nuclear medicine because of the likelihood that statistically significant results can be obtained with lower absorbed radiation dose. The tissue selectivity observed was anticipated from the pathways of catabolism of LDL and corroborated by results of the imaging experiments. Localization of radioactivity within the LDL receptor-rich liver was clearly visualized within 2 hr with  $^{68}\text{Ga}$ -DTPA-LDL and PET or with  $^{111}\text{In}$ -DTPA-LDL and gamma scintigraphy. Use of prolonged imaging times (24 hr) with the  $^{111}\text{In}$ -labeled analogue enhanced the image contrast of the metabolically active sites with liver-to-blood pool ratios exceeding 7.5. The tissue uptake of the tracers was altered by hypercholesterolemia and the consequent saturation of low-capacity LDL receptor-mediated catabolism, suggesting that  $^{68}\text{Ga}$ - and  $^{111}\text{In}$ -DTPA-LDL have potential as tracers of lipoprotein metabolism in noninvasive evaluations of tissue LDL receptor activity in pathological conditions and in their response to treatment.

## ACKNOWLEDGMENTS

The technical assistance of Debra L. Rateri and Rebecca L. Schultz is gratefully acknowledged. We also thank Dr. Robert J. Gropler and Dieter Ambos for their assistance with the PET experiments, and John C. Goble at Rensselaer Polytechnic Institute for writing software for acquisition and analysis of gamma scintigraphy data. We gratefully acknowledge the supply of dilactitol-tyramine from Dr. Suzanne R. Thorpe of the University of South Carolina. This work was supported by DOE grant DE-FG02-87ER60512 and by NIH grants

HL36822 and HL17646—Specialized Center of Research in Coronary and Vascular Diseases.

## REFERENCES

1. Lipid Research Clinics Program. The lipid research clinics coronary primary prevention trial results. I. Reduction in incidence of coronary heart disease. *JAMA* 1984;251:351–364.
2. Lipid Research Clinics Program. The lipid research clinics coronary primary prevention trial results. II. The relationship of reduction in incidence of coronary heart disease to cholesterol lowering. *JAMA* 1984;251:365–374.
3. NIH Consensus Development Conference Panel. Lowering blood cholesterol to prevent heart disease. *JAMA* 1985;253:2080–2086.
4. Brensike JF, Levy RI, Kelsey SF, et al. Effects of therapy with cholestyramine on progression of coronary arteriosclerosis: results of the NHLBI type II coronary intervention study. *Circulation* 1984;69:313–324.
5. Levy RI, Brensike JF, Epstein SE, et al. The influence of changes in lipid values induced by cholestyramine and diet on progression of coronary artery disease: results of the NHLBI type II coronary intervention study. *Circulation* 1984;69:325–337.
6. AMA Ad Hoc Committee to Design a Dietary Treatment of Hyperlipoproteinemia. Recommendations for treatment of hyperlipidemia in adults. A joint statement of the Nutrition Committee and the Council on Arteriosclerosis. *Circulation* 1984;69:1067A–1090A.
7. Goldstein JL, Brown MS. The low density lipoprotein pathway and its relation to atherosclerosis. *Ann Rev Biochem* 1977;46:897–930.
8. Mahley RW, Innerarity TL. Lipoprotein receptors and cholesterol homeostasis. *Biochim Biophys Acta* 1983;737:197–222.
9. Huettinger M, Corbett JR, Schneider WJ, Willerson JT, Brown MS, Goldstein JL. Imaging of hepatic low density lipoprotein receptors by radionuclide scintiscanning in vivo. *Proc Natl Acad Sci USA* 1989;81:7599–7603.
10. Moerlein SM, Dalal KB, Ebbe SN, Yano Y, Budinger TF. Residualizing and nonresidualizing analogues of low-density lipoprotein as iodine-123 radiopharmaceuticals for imaging LDL catabolism. *Nucl Med Biol* 1988;15:141–149.
11. Lees RS, Garabedian HD, Lees AM, et al. Technetium-99m-low density lipoproteins: preparation and biodistribution. *J Nucl Med* 1985;26:1056–1062.
12. Vallabhajosula S, Paidi M, Badimon JJ, et al. Radiotracers for low density lipoprotein biodistribution studies in vivo: technetium-99m-low density lipoprotein versus radioiodinated low-density lipoprotein preparations. *J Nucl Med* 1988;29:1237–1245.
13. Moerlein SM, Daugherty A, Welch MJ. Ga-68-DTPA-LDL: a potential radiopharmaceutical for in-vivo imaging of low-density lipoprotein receptor activity with PET [Abstract]. *J Nucl Med* 1988;29:848–849.
14. Gross MD, Skinner RWS, Schwendner SW, DeForge LE, Counsell RE, Newton RS. Indium-111-DTPA low-density lipoprotein (LDL) imaging of LDL-receptor activity [Abstract]. *J Nucl Med* 1989;30:768.
15. Rosen JM, Butler SP, Meinken GE, et al. Indium-111-labeled LDL: a potential agent for imaging atherosclerotic disease and lipoprotein biodistribution. *J Nucl Med* 1990;31:343–350.
16. Daugherty A, Oida K, Sobel BE, Schonfeld G. Dependence of metabolic and structural heterogeneity of cholesterol ester-rich very low-density lipoproteins on the duration of chole-

- terol feeding in rabbits. *J Clin Invest* 1988;82:562–570.
17. Havel RJ, Eder HA, Bragson JH. The distribution and chemical composition of ultracentrifugally separated lipoproteins in human serum. *J Clin Invest* 1955;34:1345–1353.
  18. Hnatowich DJ, Layne WW, Childs RL. The preparation of DTPA-coupled albumin. *Int J Appl Radiat Isot* 1982;33:327–332.
  19. Angelberger P, Hüttinger M, Dudczak R. Comparative study of  $^{123}\text{I}$ - and  $^{99\text{m}}\text{Tc}$ -low-density lipoproteins (LDL) [Abstract]. *J Lab Comp Radiopharm* 1986;23:1309–1311.
  20. Daugherty A, Thorpe SR, Lange LG, Sobel BE, Schonfeld G. Loci of catabolism of beta very low-density lipoprotein in vivo delineated with a residualizing label,  $^{125}\text{I}$ -dilactitol tyramine. *J Biol Chem* 1985;260:1456–1470.
  21. Loc'h C, Maziere B, Comar D. A new generator for ionic gallium-68. *J Nucl Med* 1980;21:171–173.
  22. Papadopoulos NM, Kintzios JA. Determination of human serum lipoprotein patterns by agarose gel electrophoresis. *Anal Biochem* 1969;30:421–426.
  23. Lowry OH, Roseborough NJ, Farr AL, Randall RJ. Protein measurement with the Folin phenol reagent. *J Biol Chem* 1951;193:265–275.
  24. Gropler RJ, Siegel BA, Lee KJ, et al. Nonuniformity in myocardial accumulation of F-18 fluorodeoxyglucose in normal fasted humans. *J Nucl Med* 1990;31:1749–1756.
  25. Matthews CM. The theory of tracer experiments with  $^{131}\text{I}$ -labelled plasma proteins. *Phys Med Biol* 1957;2:36–53.
  26. Strobel JL, Baynes JW, Thorpe SR. Iodine-125-glycoconjugate labels for identifying sites of catabolism in vivo: Effect of structure and chemistry of coupling to protein on label entrapment in the cell wall after protein degradation. *Arch Biochem* 1985;240:635–645.
  27. Pittman RC, Carew TE, Glass CK, Green SR, Taylor CA, Attie AD. A radioiodinated intracellularly trapped ligand for determining the sites of plasma protein degradation in vivo. *Biochem J* 1983;212:791–800.
  28. Moerlein SM, Welch MJ. The chemistry of gallium and indium as related to radiopharmaceutical production. *Int J Nucl Med Biol* 1981;8:277–287.
  29. Martell AE, Smith RM. *Critical stability constants, volume 1: amino acids*. New York: Plenum Press; 1974:284.
  30. Kita T, Brown MS, Bilheimer DW, Goldstein JL. Delayed clearance of very low density and intermediate density lipoproteins with enhanced conversion to low density lipoprotein in WHHL rabbits. *Proc Natl Acad Sci USA* 1982;79:5693–5697.
  31. Slater HR, Packard CJ, Bicker S, Shepherd J. Effects of cholestyramine on receptor-mediated plasma clearance and tissue uptake of human low-density lipoproteins in the rabbit. *J Biol Chem* 1980;255:10210–10213.
  32. Kovanen PT, Brown MS, Basu SK, Bilheimer DW, Goldstein JL. Saturation and suppression of hepatic lipoprotein receptors; a mechanism for the hypercholesterolemia of cholesterol-fed rabbits. *Proc Natl Acad Sci USA* 1981;78:1396–1400.
  33. Bratzler RL, Chisholm GM, Colton CK, Smith KA, Lees RS. The distribution of labeled low-density lipoproteins across the rabbit thoracic aorta in vivo. *Atherosclerosis* 1977;28:289–307.